



Chitosan-silver nanoparticles conjugate mediated by endophytic fungus

Talaromyces sp. 7S1: antimicrobial, antibiofilm, and anticancer

Shaimaa Faisal¹, Mohamed Emara¹, Reham M. Shawky¹, Ahmed A. Hamed^{2*}



CrossMark

¹Faculty of Pharmacy, Helwan University, Ain Helwan, Cairo, 11795, Egypt

²National Research Centre, Microbial Chemistry Department, 33 El-Buhouth Street, Dokki, Giza 12622, Egypt

Abstract

Antibiotic resistance has substantially risen worldwide. Considering this worrying condition, many studies on biogenic nanoparticles and their antimicrobial and anticancer properties have been conducted. There are numerous ways to improve stability and dispersion through conjugate peroration with bioactive natural ingredients such as chitosan. Here, a fungal isolate was isolated and identified as *Talaromyces* sp. 7S1 by 18SrRNA with accession no. OP295112. This strain prepared biogenic silver nanoparticles (AgNPs) and chitosan–AgNPs conjugate (Ch–AgNPs). Various imaging and analytical methods including UV–vis, XRD, FTIR-spectroscopy, TEM, and SEM were utilized to characterize biogenic nanoparticles and conjugates. The biosynthesized AgNPs along with the prepared conjugate were evaluated for their antimicrobial effects on Gram-positive (*Staphylococcus aureus* (RCMB 010028) and *Bacillus subtilis* (RCMB 010067)) and Gram-negative (*Escherichia coli* (RCMB 010052) and *Salmonella typhi*(RCMB 010052)) pathogens. Ch–AgNPs showed good antimicrobial activity compared to control. Results revealed that the crude extract showed antibacterial activity against *E. coli* and *S. aureus* while a substantial effect was observed with AgNPs. AgNPs displayed potent antibacterial activity against *E. coli*, *S. aureus*, and *B. subtilis*, while they showed moderate activity against *S. typhi*. Furthermore, Ch–AgNPs exhibited a pronounced antibacterial activity against *E. coli*, and *S. aureus* and low antibacterial activity against *S. typhi*. On the other hand, the obtained AgNPs and Ch–AgNPs exhibited a pronounced antibiofilm activity against all tested strains. Additionally, the antioxidant and anticancer activities of AgNPs and Ch–AgNPs were also evaluated. Collectively, AgNPs and Ch–AgNPs exhibit good antimicrobial activity, nevertheless, Ch–AgNPs conjugate reduced the toxicity of AgNPs which may represent a safer tool to inhibit bacterial pathogens.

Keywords: Chitosan-silver nanoparticles, conjugate, *Talaromyces* sp., antimicrobial, antibiofilm, anticancer

Introduction

The ubiquitous group of bacteria known as The rise and dissemination of drug-resistant pathogens, acquiring new resistance mechanisms and resulting in antimicrobial resistance, pose a continuous threat to our potential for effectively addressing prevalent diseases. Of particular concern is multi- and pan-drug resistant bacteria's rapid worldwide spread, commonly referred to as "superbugs," which could lead to infections that

cannot be treated with existing antibiotics. Unfortunately, there is a limited number of new antimicrobials in the clinical pipeline. In 2019, the World Health Organization (WHO) recognized the existence of 32 antibiotics currently in clinical development specifically targeting priority pathogens. However, out of this group, only six were regarded as groundbreaking or innovative. Additionally, the lack of access to quality antimicrobials remains a significant issue, affecting healthcare systems in countries at all levels of development. As drug

*Corresponding author e-mail: (ahmedshalbio@gmail.com).

Receive Date: 04 August 2023 Revise Date: 16 August 2023 Accept Date: 27 August 2023

DOI: 10.21608/EJCHEM.2023.227121.8361

©2024 National Information and Documentation Center (NIDOC)

resistance spreads worldwide, antibiotics are becoming less effective, leading to increased challenges in treating infections and higher mortality rates. Urgent development of new antimicrobial agents is necessary to combat resistant Gram-negative bacterial infections [1-4].

Over the past decade, nanotechnology has made significant advancements and is undergoing rapid development as a multidisciplinary scientific field. It possesses significant promise within the domain of human healthcare, providing advantages across diverse fields including the production of new drugs, water purification systems, information and communication technology, and the creation of more robust and lightweight materials [5].

Metal nanoparticles (NPs) consist of metal precursors and exhibit distinct optoelectrical properties attributed to the well-established properties of localized surface plasmon resonance (LSPR). Noble metals, such as copper (Cu), gold (Au), and silver (Ag) display a broad absorbance band in the solar spectrum's visible range. The precise synthesis of NPs of metal in terms of facets, size, and shape is critical for harnessing their advanced optical properties, enabling their application in various research fields [6]. Silver is usually acknowledged for its potent toxicity against a broad spectrum of microorganisms [7]. Numerous antibacterial applications have used silver-based compounds extensively [8, 9]. As antibacterial agents, several commercially available silver salts and derivatives are used.

Chitosan (Ch) is a linear polysaccharide obtained via deacetylating proteins from the exoskeletons of crustaceans and insects. N-acetyl-D-glucosamine and (1-4)-D-glucosamine units make up its structure. Chitosan possesses advantageous characteristics, including biocompatibility, degradability, non-toxicity, and permeability, rendering it highly valuable in the field of medicine. Chitosan finds applications in antimicrobial use, wound healing, drug delivery, biosensors, and water purification, among other biomedical uses.

To enhance its activity, Chitosan requires structural modifications, including dimensions and form alterations. These modifications can be accomplished by changing Chitosan into nanoparticle form (ranging from 1 to 1000 nanometers) using chemical, mechanical, or biological methods. The biological method is commonly employed to produce smaller chitosan nanoparticles [10]. This work aimed to

biosynthesize silver nanoparticles using fungi and explore their potential applications in antibacterial and anticancer fields.

Experimental

1.1. Sample collection and isolation of fungi

Three samples (1 seagrass, 1 soft coral, and 1 sponge) were collected using SCUBA equipment from Site (1) Abu Monqar island is located at N 27 12 53.7 and E 33 51 11.15. The samples were collected between 5 and 10 m depth in Hurghada region, Red Sea, Egypt. The three samples were frozen until used for investigation and analysis. Photos were taken underwater for each sample to show the morphology and the surrounding environment.

Isolation of associated fungi

The marine sample parts were rinsed with sterile sea water and then surface sterilized under sterile circumstances (SSW) for marine samples while normal samples were rinsed with fresh water submerged for one minute in 70% ethanol. The parts were once more sterilized by rinsing with SSW and fresh water, then 1 minute of submersion in 2% sodium hypochlorite, followed by another rinse with SSW and fresh water 3 times. Following that, 4 to 5 drops of the water from the final rinse were inoculated on potato dextrose agar medium to evaluate the effectiveness of the process of surface sterilization. The treated samples pieces were then placed on potato dextrose agar plates, approximately three weeks of incubation at 28 °C were followed by daily checks to look for the emergence of new colonies of fungi. Endophytic species should only occur on plates with organisms inoculated on them, not on plates with water rinsed off of them [11-18].

Identification of endophytes up to the species level using Qiagen DNeasy Mini Kit

Extraction of DNA

By sequencing the 18SrRNA gene, the chosen fungal strains' molecular identities were determined. Using the Qiagen DNeasy Mini Kit and adhering to the instructions in the manufacturer's manual, genomic DNA was extracted [19].

PCR amplification

The following ingredients were used in the PCR reaction mixture: 1 µg genomic DNA, 1 µL of 20 uM of each primer, 10 µM of the dNTP combination, 2 units of Taq DNA polymerase enzyme, and 10 µl of 5X reaction buffer. Two primers were used for the

amplification processes; ITS1 (5'-TCCGTAGGTGAACCTGCG-3')/ ITS4 (5'-TCCTCCGCTTATTG ATATGC-3'). A step of denaturation at 94 °C for 5 min, 35 cycles of 94 °C for 30 sec, 55 °C for 30 sec, 72 °C for 90 min, and a final extension step at 72 °C for 5 min were employed in the PCR [19-23].

Sequencing

The amplified products were purified and sequenced in South Korea's Macrogen Companies. The generated sequence was examined using the BLAST software to compare its similarity and homology to other similar existing sequences found in the NCBI database.

Preparation of fungal culture filtrate

Small-scale fermentation was performed in 250 mL flasks using a potato dextrose broth medium. For the liquid medium, the fungal culture was inoculated into 50 mL of 250 Erlenmeyer flask for 7 days at 28°C at 120 rpm. After incubation, the cells were separated from the culture supernatants by 6,000 rpm, 10-minute centrifugation at 6 °C [10].

Biosynthesis of AgNPs

The ability of the obtained fungus to biosynthesize AgNO₃ aqueous solution (1.0 mM) was combined with 25 mL of fungal supernatants to create AgNPs. The mixture was incubated in a dark, 200-rpm rotary shaker at 32 °C for five days. The synthesis process was done in a similar manner utilizing the cell filtrate under similar circumstances. It was decided to examine each ingredient's effectiveness in producing AgNPs by employing both bacterial supernatant and cell filtrates in the biosynthesis process. A control experiment was conducted by combining AgNO₃ solution and an un-inoculated culture medium (fungi broth as control), demonstrating the involvement of acquired fungus in the biosynthesis of AgNPs. Upon incubation with a fungal supernatant, the AgNO₃ solution's color transitioned from colorless to yellowish-brown [10].

Preparation of Chitosan–AgNPs

Chitosan-AgNP conjugate synthesis was performed as previously described [18]. In a nutshell, a commercial grade 0.5% (w/v) chitosan solution was ultrasonically dispersed and dropped into a 5.0% (w/v) acetic acid solution for 1 h at 28 ± 2 °C while being stirred. The degree of deacetylation (DDA) was 88.3%. Drop by drop, 10% (w/v) of biogenic AgNPs were added. They

were then extruded into a 20 mL chitosan solution and constantly spun at 120 rpm. After the initial mixture preparation, a 0.5% (w/v) glutaraldehyde solution was introduced to the mixture. This solution was freshly prepared in a 50 mM Na-malonate buffer with a pH of 4.5. The activation process was carried out for an additional 2.0 hours. Subsequently, the activated mixture was transferred into a sterile Petri dish, properly labeled, and then placed in a hot air oven at 50 °C. The incubation was allowed to proceed for 24 hours to facilitate the development of chitosan-AgNP conjugates.

Characterization of Biosynthesized AgNPs and Chitosan–AgNPs

UV–Vis Spectral Analysis

AgNPs biosynthesis was initially detected as a change in the color of the solution. With the help of a Spectrostar nano absorbance plate reader (**BMG LABTECH GmbH, Allmendgrun, Germany**), aliquots (1 mL) of the mixture were taken to trace the transformation.

Studies of X-ray Diffraction (XRD)

Utilizing a PAN analytical X'pert PRO X-ray diffractometer (Philips, Eindhoven, Netherlands), we employed Cu Kα1 radiation and operated at around 40 kV and 30 mA to investigate the X-ray diffraction (XRD) pattern of the freshly synthesized silver nanoparticles (AgNPs). The XRD data was collected in the 2θ range of 10° to 80°, with a scanning rate of 0.02°/min. Before analysis, the sample was drop-coated onto a glass substrate to ensure accurate measurements.

Fourier-Transform Infrared Spectroscopy (FTIR)

According to Brock-Neely (1957), AgNPs spectra were obtained using the Broker vertex 80 v in the 4000-400 cm⁻¹ region with a resolution of 4 cm⁻¹.

Electron Microscopy Analysis

The produced AgNPs and Chitosan–AgNPs size and shape were examined using transmission and scanning electron microscopy (TEM) at the National Research Centre, Egypt. For TEM, the sample preparation was carried out onto copper grids that had been coated with carbon, while 2-4 μL of a silver nanoparticle solution was applied. A Philips 10 Technai with a wavelength (λ) of 0.0251 and an accelerating voltage of roughly 180 keV was used to detect the thin films after they had been air-dried. The Scanning Electron Microscope (SEM) is an advanced imaging device that employs a

concentrated electron beam to examine the fine surface details and structure of samples at high resolution. Through the generation of secondary and backscattered electrons, the SEM offers valuable insights into the sample's composition, elemental makeup, and other characteristics. Proper sample preparation is necessary, and the SEM operates within a high-vacuum environment to reduce electron scattering. Its ability to produce detailed grayscale images facilitates precise analysis, rendering it an indispensable tool across a wide range of scientific disciplines, including materials science, nanotechnology, biology, and geology.

Biological activity

Antimicrobial Assay

In 96-well flat polystyrene plates, the nanoparticles' antibacterial activity was evaluated against (*Staphylococcus aureus* (RCMB 010028) and *Bacillus subtilis* (RCMB 010067)) and Gram-negative (*Escherichia coli* (RCMB 010052) and *Salmonella typhi*(RCMB 010052)). The test extracts were added to 80 μ L of lysogeny broth (LB broth), 10 μ L of bacterial culture suspension (log phase), and 10 μ L of test extracts (final concentration of 50 μ g/ml) before the plates were incubated at 37 °C overnight. Using a Spectrostar Nano Microplate Reader (BMG LABTECH GmbH, Allmendgrun, Germany), the absorbance was measured after 20 hours at OD600 to determine the antibacterial activity [24, 25].

Antibiofilm Assay

We tested the biofilm-inhibitory effectiveness of the extracts against four clinical isolates namely, *S. aureus*, *B. subtilis*, *P. aeruginosa*, and *E. coli* using 96-well flat polystyrene plates. In brief, 180 μ L of lysogeny broth (LB broth) was poured into each well, followed by 10 μ L of pathogenic bacteria, 10 μ L of samples, and control (with a final concentration of 500 μ g mL⁻¹) (without test sample). To get rid of any free-floating bacteria, the plates were incubated for 24 hours at 37°C before the contents of the wells were removed and washed with 200 μ L of phosphate buffer saline (PBS), pH 7.2, following that, it was dried for 1 hour in sterile laminar flow, each well received 200 μ L of 0.1% (w/v) crystal violet for staining; the excess stain was removed, and the plates were then allowed to dry. Using a Spectrostar Nano Microplate Reader at 570 nm, the optical density was assessed after washing the dried plates with 95% ethanol. (BMG LABTECH GmbH, Germany's Allmendgrun).

Antioxidant activity

The antioxidant activity was carried out using phosphomolybdenum assay. The assay performed based on the reduction of molybdenum (VI) to molybdenum (V) via the interaction with the tested sample and subsequent formation of a green-colored [phosphate=Mo (V)] complex at an acidic medium with maximal absorption at 695 nm [9].

The effects of cytotoxicity are assessed using a variety of cell lines

For the cytotoxicity test, three cell lines (breast cancer of the mammary gland (MCF-7), Renal Cell Carcinoma (UO-31) and hepatocellular carcinoma (Hep-G2) were planted in 96-well plates at a cell concentration of 1×10^4 cells per well in 100 μ l of growth medium. The viability percentage was measured as $[(OD_t/OD_c)] \times 100\%$ where OD_t represents the average optical density of wells treated with the test sample and OD_c represents the average optical density of cells that were not treated [26-31].

Results

Marine sample collection

The fungal isolate coded as 7S1 was obtained from the sea grass *Thalassia hemprichii*. The obtained fungus was purified and kept in glycerol stock at -20°C until further investigation.

Identification of isolated fungus

Morphological identification of fungus

In ten days, colonies reaching 3-4 cm at 28 °C, white, ochraceous buff to cream buff, reverse yellow buff to brown in age. Globose conidial heads loosely radiate. Conidia are sub-spherical, measuring 3.5 μ m in diameter and 6 μ m in diameter, respectively.

Genetic identification

Based on the initial assessment of the isolated fungus according to UV absorbance, the isolated fungal strain 7S1 was selected and detected using the 18S rRNA gene's sequencing. The 7S1 isolate's DNA was isolated, determined and compared to other known sequences in the GenBank database determining the similarity score and statistical significance of the matches using the BLAST program (<http://www.blast.ncbi.nlm.nih.gov/Blast>, accessed on January 25, 2022). The outcomes showed that the isolate 7S1's 18S rRNA gene sequences were 100% identical to those of *Talaromyces* sp. Therefore, the selected isolate was deposited in the GenBank as *Talaromyces* sp. 7S1 and was assigned the accession number OP295112. Using the Neighbor-Joining

approach, the evolutionary history was inferred. In the most promising tree, the branches are accompanied by a percentage of duplicate trees showing how the connected taxa clustered during the bootstrap test (500 repetitions) (**Fig. 1**). The final dataset contained 998 locations altogether. In MEGA X, evolutionary analyses were carried out.

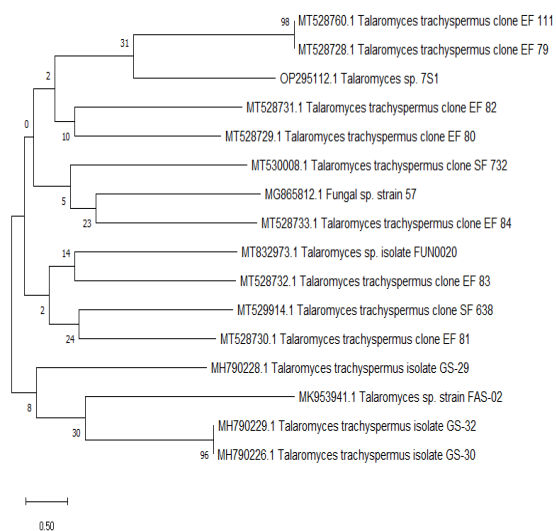


Fig. 1. Evolutionary tree of Fungal isolate 7S1

Biosynthesis of AgNPs and Biogenic Chitosan–AgNPs

AgNPs were biosynthesized using a fungal filtrate, confirming its involvement as the AgNO₃ solution changed from colorless to yellowish-brown upon incubation with fungal supernatant. The chitosan-AgNPs conjugate was prepared by dispersing a 0.5% (w/v) chitosan solution ultrasonically and gradually adding it dropwise to a 5.0% (w/v) acetic acid solution at 28 ± 2 °C with stirring. The degree of deacetylation (DDA) of chitosan was determined to be 88.3%. Subsequently, 10% (w/v) biogenic AgNPs were incorporated into the chitosan solution while continuously spinning at 120 rpm. Chitosan nanoparticle is an emerging field of research that has been gaining considerable attention in recent years due to its potential applications in various industries. Chitosan, a biopolymer derived from chitin, has several unique properties such as biocompatibility, biodegradability, and non-toxicity, which makes it an excellent candidate for developing nanoparticles. Chitosan nanoparticles have a high surface area to volume ratio, which makes them an efficient drug carrier, and they can easily penetrate cell membranes due to their small size, which enhances drug delivery.

Additionally, chitosan nanoparticles have antimicrobial properties and can be used as a natural preservative in the food industry. They can also be used to remove heavy metals from wastewater due to their excellent adsorption capacity. Furthermore, chitosan nanoparticles have applications in agriculture for plant growth promotion and disease prevention. In summary, chitosan nanoparticles have significant potential in various fields and are expected to have a significant impact on society in the near future [10]

Characterization of Talaromyces sp. 7S1 AgNPs and Biogenic Chitosan–AgNPs

Electron microscopy

Talaromyces sp. 7S1. Cell-free extract induced the formation of AgNPs. The 400 to 550 nm surface plasmon resonance (SPR) absorption spectra showed that AgNPs were produced at various periods. Field emission scanning electron microscopy (FESEM) and transmission electron microscopy (TEM) were used to investigate the measurements and morphology of the green AgNPs. The average particle size of the AgNPs was around 6.0 ± 35 to 50.0 ± 74, according to the TEM micrograph, the particle was shaped like a sphere. (**Fig. 2-5**). Additionally, the morphology of Ch-AgNPs conjugate was also visualized using TEM (**Fig. 2 and 4**) and (FESEM) (**Fig. 3 and 5**)

X-ray diffraction (XRD)

The X-ray diffraction (XRD) patterns of the chitosan–silver nanoparticles (AgNPs) are presented in **Figure 6**, offering crucial insights into the structural composition of the synthesized material. The XRD pattern of the chitosan–AgNPs prominently featured a robust characteristic peak for chitosan at approximately 10°. Notably, the XRD analysis also revealed additional peaks at around 38°, 44°, 64° and 77°, corresponding specifically to the presence of silver nanoparticles in conjunction with the chitosan matrix. This distinct pattern showcases the successful integration of chitosan with silver nanoparticles, with the chitosan maintaining its characteristic peak at 10°. The detailed XRD analysis provides a comprehensive understanding of the crystalline structure of the chitosan–AgNPs composite, shedding light on the unique properties and potential applications of this synthesized material.

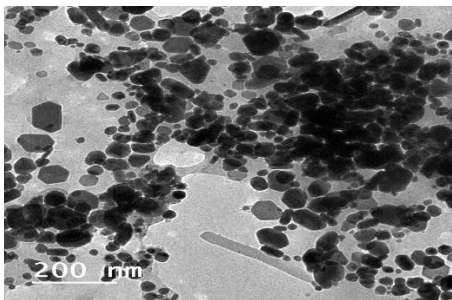


Fig. 2. Transmission electron micrograph of 7S1 AgNPs

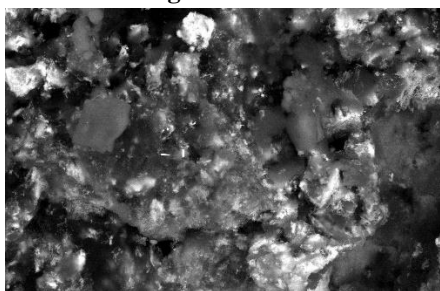


Fig. 3. Scan electron micrograph of 7S1 AgNPs

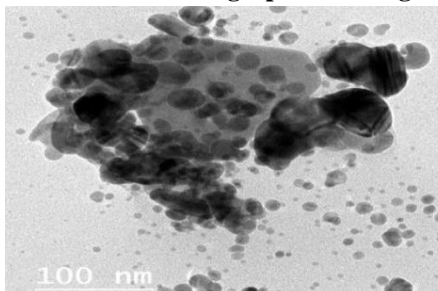


Fig. 4. Transmission electron micrograph of Ch-AgNPs

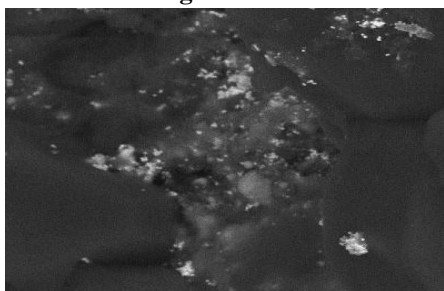


Fig. 5. Scan electron micrograph of Ch-AgNPs

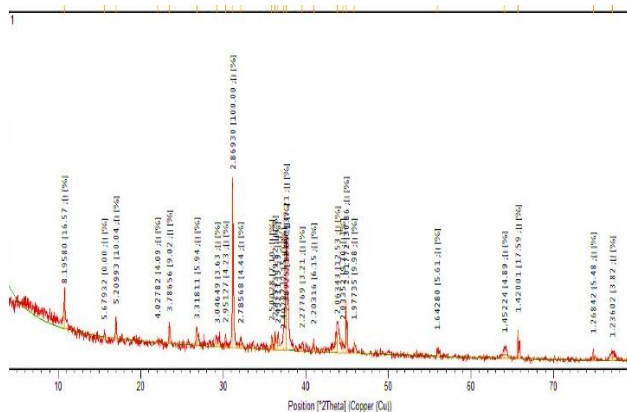


Fig. 6. XRD pattern for AgNPs

Fourier transforms infrared spectroscopy analysis (FTIR)

To determine the functional groups responsible for the production and stability of silver nanoparticles, FTIR was used. Spectral data from the FTIR of the fungal crude extract revealed that peaks at 3300, 2850, 1700, 1300, 1200 cm^{-1} according to various functional groups, among them are OH, C=O, C-O, C-N, and C-C. in prepared nanoparticles (**Fig. 7**). On the other hand, the AgNPs FTIR profile revealed that, the hydroxyl group stretching vibration peaks disappear from the spectra (**Fig. 8**). The disappearance of this peak may result from the reaction and formation of AgNPs. Additionally, the decrease of the Ag metal ions and the stability of the produced AgNPs are both significantly influenced by the presence of these functional groups in the crude extract.

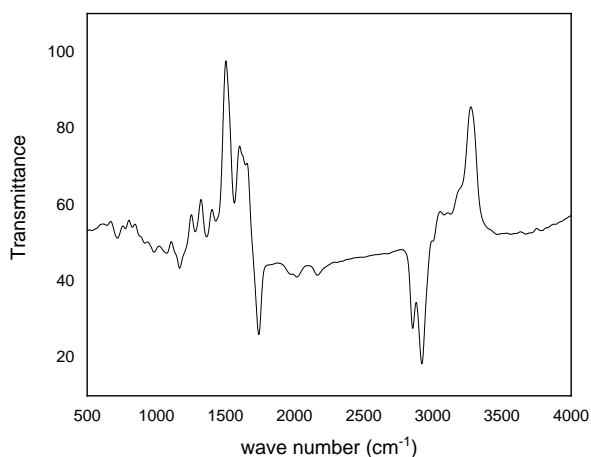


Fig. 7. FTIR of the 7S1 crude extract

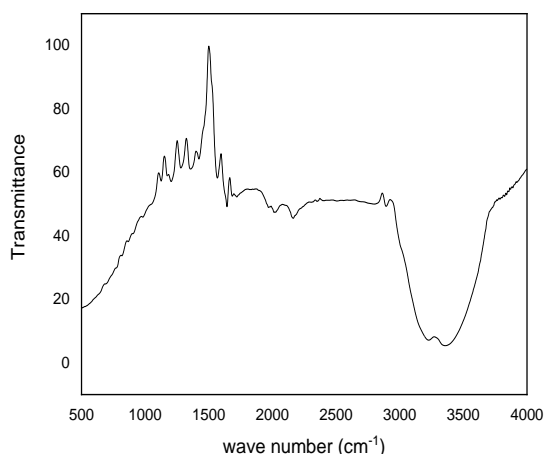


Fig. 8. FTIR of the 7S1 AgNPs extract demonstrating the Disappearance of hydroxyl group stretching vibration peaks from the spectra

Biological evaluation

Antimicrobial activity

Antimicrobial resistance (AMR) is a pressing issue, especially considering bacterial antibiotic resistance. Bacteria have gradually, and to varied degrees, become resistant to every new antibiotic that enters the market. Given this situation, it is critical to take action to prevent a growing global healthcare disaster [1]. Widely studied polymeric nanoparticles have demonstrated benefits such as high biocompatibility, prolonged release, targeting, and increased bioavailability as carriers for building antimicrobial agent delivery systems [7]. 96-well flat polystyrene plates were used to test the antibacterial activity of the *Talaromyces* sp. 7S1 axenic crude extract, biosynthesized AgNPs, and Ch-AgNPs against pathogenic bacteria and fungi. The obtained results demonstrated that the crude extract was solely effective against *S. aureus* and *E. coli* in terms of antibacterial activity. while there was a significant increase in the inhibition ratio when the biosynthesized AgNPs were used. AgNPs showed strong antibacterial action against *E. coli*, *S. aureus*, and *B. subtilis*, but *S. typhi* only showed moderate antibacterial activity. Additionally, Ch-AgNPs showed strong antibacterial action against *S. aureus* and *E. coli*, but very weak antibacterial activity against *S. typhi*. (Tables 1 and 2). Furthermore, two fungi, *Candida albicans* and *Aspergillus niger*, are susceptible to the antifungal action. The obtained results showed that the crude extract did not show any activity, while the obtained AgNPs and Ch-AgNPs

showed a pronounced activity against tested strains (Tables 3 and 4). The Minimum inhibitory concentrations for positive strains were estimated and presented in (Tables 3 and 4). Overall, the formed AgNPs and Ch-AgNPs showed a promising MIC toward most tested microbes.

Table 1. Antibacterial activity of tested nanoparticles

Tested compound	Inhibition ratio (%)			
	<i>S. typhi</i>	<i>B. subtilis</i>	<i>S. aureus</i>	<i>E. coli</i>
Crude extract	0	0	65	32.5
AgNPs	49.05	60.5	65.43	71.60
Ch-AgNPs	25.26	52.12	66.23	62
Ciprofloxacin	98	-	96	98

Table 2. Minimum inhibitory concentrations of tested nanoparticles against bacterial pathogens

Tested compound	MIC ($\mu\text{g/ml}$)			
	<i>S. typhi</i>	<i>E. coli</i>	<i>S. aureus</i>	<i>B. subtilis</i>
Crude extract	0	15.62	15.62	0
AgNPs	15.62	7.81	3.90	15.62
Ch-AgNPs	62.50	7.81	3.90	7.81
Ciprofloxacin	-	0.390	1.25	3.25

Table 3. Antifungal activity

Tested compound	Inhibition ratio (%)	
	<i>C. Albicans</i>	<i>A. niger</i>
Crude extract	0	0
AgNPs	65.00	75.02
Ch-AgNPs	62.25	69.025
Nystatin	97	98

Table 4. Minimum inhibitory concentrations of tested compounds against fungal pathogens

Tested compound	MIC ($\mu\text{g/ml}$)	
	<i>A. niger</i>	<i>A. flavus</i>
AgNPs	15.62	7.81
Ch-AgNPs	7.81	7.81
Nystatin	20.0	8.25

Anti-biofilm activity

Biofilm formation is a crucial virulence factor in many microorganisms responsible for chronic infections. These biofilms consist of intricate structures enclosed within an extracellular polymeric substance (EPS) composed of polysaccharides, proteins, and DNA [32]. This complexity allows bacteria to adhere to medical devices or injured tissue, leading to persistent infections [33]. Within biofilm formation, EPS plays a significant role in resisting antibiotics by hindering their diffusion and penetration due to the acidic pH and lower oxygen levels. Approximately 80% of the bacterial biomass within biofilms contributes to the generation of multi-drug resistant (MDR) bacteria [34, 35]. Both Gram-positive and Gram-negative bacteria, such as *S. aureus* and *E. coli*, are capable of forming biofilms. In this study, we evaluated the antibiofilm activities of the prepared AgNPs and Ch-AgNPs conjugate against four pathogenic bacteria, including *P. aeruginosa*, *S. aureus*, *E. coli*, and *B. subtilis*, using the MTT assay. The results revealed that the crude extract exhibited moderate antibiofilm activity against *S. aureus* but showed relatively lower activity against the other tested pathogens. In contrast, the obtained AgNPs and Ch-AgNPs demonstrated pronounced activity against all the tested strains (Table 5).

Table 5. The biofilm inhibition ratio of *Talaromyces sp. 7S1* crude, AgNPs and Biogenic Chitosan–AgNPs

Pure extract	Biofilm inhibition ratio%			
	<i>E. coli</i>	<i>S. aureus</i>	<i>B. subtilis</i>	<i>P. aeruginosa</i>
Crude extract	35.32	56.14	11.25	25.25
AgNPs	71.14	61.8	71.54	66.11
Ch-AgNPs	63.62	70.52	50.49	65.61

Antioxidant activity

The antioxidant activity was carried out using phosphomolybdenum assay which is based on the reduction of molybdenum (VI) to molybdenum (V) via the interaction with the tested sample and subsequent formation of a green-colored [phosphate=Mo (V)] complex at acidic medium with a maximal absorption at 695 nm [9]. The results presented in Table 6 showed that the TAC of *Talaromyces sp. 7S1* crude extract is 434.06 ± 1.54 mg AAE/g. On the other hand, the AgNPs exhibited antioxidant capacity up to 325.32 ± 3.07 mg AAE/g followed by Ch-AgNPs which showed antioxidant activity 299.13 ± 4.69 mg AAE/g.

Table 6. Total antioxidant capacity (TAC) for *Talaromyces sp. 7S1* crude, AgNPs and Biogenic Chitosan–AgNPs

Pure compounds	Total antioxidant capacity (mg AAE/g compound) ^{1,2}
Cr	434.06 ± 1.54
AgNPs	325.32 ± 3.07
Ch-AgNPs	299.13 ± 4.69

Anticancer activity

The anticancer activity of the prepared AgNPs and Ch-AgNPs conjugate was measured against three cell lines (breast cancer of the mammary gland (MCF-7), Renal Cell Carcinoma (UO-31), and hepatocellular carcinoma (Hep-G2)). Results showed that the biosynthesized AgNPs showed an IC₅₀ value of 95.09 ± 4.7 µg/ml against hepatocellular carcinoma (Hep-G2), while the Ch-AgNPs showed good anticancer activity against Hep-G2 with an IC₅₀ value of 21.85 ± 1.1 µg/ml for hepatocellular carcinoma (Table 7). For Renal Cell Carcinoma (UO-31), the AgNPs showed low anticancer activity against UO-31 with an IC₅₀ value of 86.58 ± 4.3 µg/ml, while Ch-AgNPs displayed potent anticancer activity with IC₅₀ 6.42 ± 0.3 µg/ml against UO-31. Furthermore, the obtained results for breast carcinoma showed that AgNPs showed moderate anticancer activity against MCF-7 with IC₅₀ of 33.79 ± 1.7 µg/ml while Ch-AgNPs displayed potent anticancer activity with IC₅₀ 11.77 ± 0.6 µg/ml against MCF-7 cell line. The Staurosporine was used as a control.

Table 7. Anticancer activity of *Talaromyces sp. 7S1* crude, AgNPs, and Biogenic Chitosan–AgNPs against different cell lines

Sample	Cytotoxicity (IC ₅₀ , µg/ml)		
	HepG2	UO-31	MCF7
AgNPs	95.09 ± 4.7	86.58 ± 4.3	33.79 ± 1.7
Ch-AgNPs	21.85 ± 1.1	6.42 ± 0.3	11.77 ± 0.6
Staurosporine	5.73 ± 0.3	8.01 ± 0.4	10.11 ± 0.5

Conclusion

The use of fungal extracts for the biogenic synthesis of silver nanoparticles was found to be an efficient, cost-effective, and secure method based on the results obtained. Additionally, the Ch-AgNPs conjugates

demonstrated bioactive potentialities, such as antibacterial capabilities against the examined microorganisms where Ch-AgNPs also exhibited antibacterial activity. The effectiveness of utilizing Ch-AgNPs for antibiofilm activity against specific pathogenic species also strongly suggests the superiority of using AgNP, which may be caused by a greater plasmon resonance in the silver nanoparticle. Additionally, the anticancer activity of AgNPs and Ch-AgNPs was assessed in relation to several cell lines, with the results demonstrating that Ch-AgNPs demonstrated strong anticancer activity with an IC₅₀ of 6.420.3 g/ml against UO-31.

Conflicts of interest: "There are no conflicts to declare"

Acknowledgement: Supports of this work provided by national research center (NRC) and benha university, faculty of science. for the facilities provided.

References

- [1] Ventola, C. L., The antibiotic resistance crisis: part 2: management strategies and new agents. *P T* 40(5): 344-352 (2015).
- [2] Zayed, K.M., Ghareeb, M.A., Habib, M.R., et al., Biological activity, chemical profiling and molecular docking of tissue extracts of the sea snail *Trochus erithreus*. *Journal of Applied Pharmaceutical Science* this link is disabled, 2023, 13(6), pp. 199–210
- [3] El-Bendary M.A., Afifi S.S., Moharam M.E., Abo El-Ola S.M., Salama A., Omara E.A., Shaheen M.N.F., Hamed A.A. and Gawdat N.A., Biosynthesis of silver nanoparticles using isolated *Bacillus subtilis*: characterization, antimicrobial activity, cytotoxicity, and their performance as antimicrobial agent for textile materials, *Prep Biochem Biotechnol.*, 51, 54-68 (2020).
- [4] Abdel-Monsef, M.M., Darwish, D.A., Zidan, H.A., Hamed, A.A., Ibrahim, M.A. Characterization, antimicrobial and antitumor activity of superoxide dismutase extracted from Egyptian honeybee venom (*Apis mellifera lamarckii*). *Journal of Genetic Engineering and Biotechnology* this link is disabled, 2023, 21(1), 21
- [5] Williams, D., Nanotechnology: a new look." *Medical device technology* 15: 9-10 (2004).
- [6] Dreaden, E. C., A. M. Alkilany, et al., The golden age: gold nanoparticles for biomedicine. *Chem Soc Rev* 41(7): 2740-2779 (2012).
- [7] Liao, S. Y., D. C. Read, et al., Interaction of silver nitrate with readily identifiable groups: relationship to the antibacterial action of silver ions. *Lett Appl Microbiol* 25(4): 279-283(1997).
- [8] Gupta, A. and S. Silver., Silver as a biocide: will resistance become a problem?" *Nat Biotechnol* 16(10): 888(1998).
- [9] Nomiya, K., A. Yoshizawa, et al., Synthesis and structural characterization of silver(I), aluminium(III) and cobalt(II) complexes with 4-isopropyltropolone (hinokitiol) showing noteworthy biological activities. Action of silver(I)-oxygen bonding complexes on the antimicrobial activities." *J Inorg Biochem* 98(1): 46-60 (2004).
- [10] Mostafa, E. M., M. A. Abdelgawad, et al., Chitosan Silver and Gold Nanoparticle Formation Using Endophytic Fungi as Powerful Antimicrobial and Anti-Biofilm Potentialities. *Antibiotics (Basel)* 11(5) (2022).
- [11] Buseti, A., G. Shaw, et al., Marine-derived quorum-sensing inhibitory activities enhance the antibacterial efficacy of tobramycin against *Pseudomonas aeruginosa*. *Mar Drugs* 13(1): 1-28(2014).
- [12] Abdel-Aziz M.S., Ghareeb M.A., Saad A.M., Refahy L.A. and Hamed A.A., Chromatographic isolation and structural elucidation of secondary metabolites from the soil-inhabiting fungus *Aspergillus fumigatus* 3T-EGY, *Acta Chromatogr*, 30, 243-249 (2018).
- [13] Aly S., Hathout A., El-Nekeety A., Hamed A., Sabry B., Abdel-Aziz M. and Ghareeb, M., Egyptian bacterial exhibiting antimicrobial and antiaflatoxigenic activity *J. Appl. Pharm. Sci*, 6, 001-010 (2016).
- [14] Aly S.E., Abdel-Wahhab M.A., El-Neekety A.A., Abdel-Aziz M.S., Hathout A.S., Hamed A.A., Sabry B.A. and Ghareeb M.A., Molecular identification of newly isolated non-toxicogenic fungal strains having antiaflatoxigenic, antimicrobial and antioxidant activities, *Der Pharma Chem*, 8, 121-134 (2016).
- [15] Elawady M.E., Hamed A.A., Alsallami W.M., Gabr E.Z., Abdel-Monem M.O., Hassan M.G., Bioactive Metabolite from Endophytic *Aspergillus versicolor* SB5 with Anti-Acetylcholinesterase, Anti-Inflammatory and Antioxidant Activities: In Vitro and In Silico Studies. *Microorganisms*. 2023; 11(4):1062. <https://doi.org/10.3390/microorganisms11041062>
- [16] Hamed A.A. Soldatou S., Qader M.M., Arjunan S., Miranda K.J., Casolari F., Pavesi C., Diyaolu O.A., Thissera B., Eshelli M., Belbahri L., Luptakova L., Ibrahim N.A., Abdel-Aziz M.S., Eid B.M., Ghareeb M.A., Rateb M.E. and Ebel R., Screening fungal endophytes derived from under explored Egyptian marine habitats for antimicrobial and antioxidant properties in factionalised textiles, *Microorganisms*. 8, 1617 (2020).

- [17] Khazaal HT, Khazaal MT, Abdel-Razek AS, Hamed AA, Ebrahim HY, Ibrahim RR, Bishr M, Mansour YE, El Dib RA, Soliman HSM. Antimicrobial, antiproliferative activities and molecular docking of metabolites from *Alternaria alternata*. *AMB Express*. 2023 Jul 6;13(1):68. doi: 10.1186/s13568-023-01568-1. PMID: 37414961; PMCID: PMC10326215.
- [18] El-Ghorab A.H., Behery F.A., Abdelgawad M.A., Alsohaimi I.H., Musa A., Mostafa E.M., Altaleb H.A., Althobaiti I.O., Hamza M., Elkomy M.H., et al. LC/MS Profiling and Gold Nanoparticle Formulation of Major Metabolites from *Origanum majorana* as Antibacterial and Antioxidant Potentialities. *Plants*. 11(14):1871(2022). <https://doi.org/10.3390/plants11141871>
- [19] Hamed A.A., Abdel-Aziz M.S., Fadel M. and Ghali M.F., Antidermatophytes from bioactive secondary metabolites of local *Streptomyces* spp. *J. Innov. Pharm. Biol. Sci.* 3, 155-165 (2016).
- [20] Hamed A.A., Abdel-Aziz M.S., Fadel M., et al., Antimicrobial, antidermatophytic, and cytotoxic activities from *Streptomyces* sp. MER4 isolated from Egyptian local environment. *Bulletin of the National Research Centre*, 42 (1), 1-10(2018).
- [21] Hamed A.A., Kabary H., Khedr M. and Emam A.N., Antibiofilm, antimicrobial and cytotoxic activity of extracellular green-synthesized silver nanoparticles by two marine-derived actinomycete., *RSC Adv.*, 10, 10361-10367 (2020).
- [22] Hifnawy M.S., Hassan H.M., Mohammed R., Fouda M.M., Sayed A.M., Hamed A.A., AbouZid S.F., Rateb M.E., Alhadrami H.A. and Abdelmohsen, U.R., Induction of antibacterial metabolites by co-cultivation of two Red-Sea sponge-associated actinomycetes *micromonospora* sp. UR56 and *Actinokinespora* sp. EG49., *Mar. Drugs*, 18, 243 (2020).
- [23] Mohamed, S.S., El Awady, M.E., Abdelhamid, S.A., et al., Study of exopolysaccharide produced by *Streptomyces rochie* strain OF1 and its effect as ameliorative on osteoarthritis in rats via inhibiting TNF- α /COX2 pathway. *Journal of Genetic Engineering and Biotechnology* this link is disabled, 2023, 21(1), 12
- [25] Eskander D.M., Atalla S.M.M., Hamed A.A., ElKhrisy E.D.A. Investigation of Secondary Metabolites and its Bioactivity from *Sarocladium kiliense* SDA20 Using Shrimp Shell Wastes, *Pharmacogn. J.*, 12, 636-644 (2020).
- [26] Musa A, Abdelgawad MA, Shaker ME, El-Ghorab AH, Parambi DGT, Hamed AA, Sayed AM, Hassan HM, Aboseada MA. Screening and Molecular Docking of Bioactive Metabolites of the Red Sea Sponge *Callyspongia siphonella* as Potential Antimicrobial Agents. *Antibiotics*. 2022; 11(12):1682. <https://doi.org/10.3390/antibiotics11121682>
- [26] Abd El-Hady F.K., Shaker K.H., Souleman A.M.A., Fayad W., Abdel-Aziz M.S., Hamed A.A., Iodice C. and Tommonaro G., Comparative Correlation Between Chemical Composition and Cytotoxic Potential of the Coral-Associated Fungus *Aspergillus* sp. 2C1-EGY Against Human Colon Cancer Cells. *Curr. Microbiol*, 74, 1294-1300 (2017).
- [27] Abdel-Aziz M.S., Hathout A.S., El-Neleety A.A., Hamed A.A., Sabry B.A., Aly S.E and Abdel-Wahhab, M.A., Molecular identification of actinomycetes with antimicrobial, antioxidant and anticancer properties, *Comun. Sci*, 10, 218-231 (2019).
- [28] AboElmaaty S.A., Shati A.A., Alfaifi M.Y., Elbehairi S.E.I., Sheraba N.S., Hassan M.G., Badawy M.S.E.M., Ghareeb. A., Hamed A.A., Gabr E.Z., Biofilm Inhibitory Activity of Actinomycete-Synthesized AgNPs with Low Cytotoxic Effect: Experimental and In Silico Study. *Microorganisms*. 2022 Dec 30;11(1):102. doi: 10.3390/microorganisms11010102. PMID: 36677395; PMCID: PMC9866079.
- [29] Elkhoully H.I., Hamed A.A., El Hosainy A.M., Ghareeb M.A., Sidkey N.M., Bioactive secondary metabolite from endophytic *Aspergillus tubenginses* ASH4 isolated from *Hyoscyamus muticus*: antimicrobial, antibiofilm, antioxidant and anticancer activity. *Pharmacognosy Journal*, 13(2), 434- 424(2021). DOI: 10.5530/pj.2021.13.55.
- [30] Ghareeb M.A., Hamed M.M., Saad A.M., AbdelAziz M.S., Hamed A.A. and Refahy L.A., Bioactive secondary metabolites from the locally isolated terrestrial fungus. *Penicillium* sp. SAM16-EGY. *Pharmacogn., Res.*, 11, 162-170 (2019).
- [31] Hussein, M., El-Senousy, A., El-Askary, H., El Fishawy, A., Hamed, A., Youness, R. 'Pseurotin A Halts Hepatocellular Carcinoma Oncogenic Potential Through Tuning miR-30a and let-7i Tumor Suppressor miRNAs', *Egyptian Journal of Chemistry*, 65(131), pp. 501-509 (2022). doi: 10.21608/ejchem.2022.141384.6186
- [32] Anjugam, M., B. Vaseeharan, et al., Biological synthesis of silver nanoparticles using beta-1, 3 glucan binding protein and their antibacterial, antibiofilm and cytotoxic potential." *Microb Pathog* 115: 31-40(2018).
- [33] Rajivgandhi, G., R. Vijayan, et al., Antibiofilm effect of *Nocardiosis* sp. GRG 1 (KT235640) compound against biofilm forming Gram negative bacteria on UTIs. *Microb Pathog* 118: 190-198 (2018).
- [34] Singh, S., S. Datta, et al., Bacterial exo-polysaccharides in biofilms: role in antimicrobial resistance and treatments. *J Genet Eng Biotechnol* 19(1): 140 (2021).
- [35] de Brito, F. A. E., A. P. P. de Freitas, et al., Multidrug-Resistant Biofilms (MDR): Main Mechanisms of Tolerance

and Resistance in the Food Supply Chain. *Pathogens* 11(12) (2022).

[36] K. Stritzke, S. Schulz, H. Laatsch, E. Helmke, and W. Beil, "Novel caprolactones from a marine streptomycete," *J Nat Prod*, vol. 67, no. 3, pp. 395–401, Mar. 2004, doi: 10.1021/np030321z.